Molecular Pharmacology Fast Forward. Published on May 24, 2005 as DOI: 10.1124/mol.105.011957

Spatial orientation of the antagonist granisetron in the ligand-binding site of the 5-HT_3 receptor

Dong Yan and Michael M. White
Department of Pharmacology & Physiology
Drexel University College of Medicine
245 N. 15th Street
Philadelphia, PA 19102-1192

Running Title: Antagonist orientation in 5-HT_{3A}R Binding Site

Corresponding Author:

Michael M. White, Ph.D.
Department of Pharmacology & Physiology
Drexel University College of Medicine
245 N. 15th Street
Philadelphia, PA 19102

Phone: (215) 762-4530
Fax: (215) 762-4850
e-mail: mikewhite@drexel.edu

Number of text pages: 19

Number of Tables: 2

Number of figures: 5

Number of references: 40

Number of words in the Abstract: 235

Number of words in the Introduction: 688

Number of words in the Discussion: 1062

Non-standard abbreviations:

AChBP: acetylcholine binding protein

5-HT_{3A}R: homomeric 5-HT_{3A} subunit-containing 5-HT_3R

LGIC: cys-loop ligand gated ion channel

Molecular Pharmacology Fast Forward. Published on May 24, 2005 as DOI: 10.1124/mol.105.011957
This article has not been copyedited and formatted. The final version may differ from this version.

ABSTRACT

The serotonin type 3 receptor (5-HT_3R) is a member of the cys-loop ligand-gated ion channel (LGIC) superfamily. Like almost all membrane proteins, high-resolution structural data are unavailable for this class of receptors. We have taken advantage of the high degree of homology between LGICs and the ACh binding protein (AChBP) from the freshwater snail *Lymnea*, for which high-resolution structural data are available, to create a structural model for the extracellular (*i.e.*, ligand-binding) domain of the 5-HT_3R and to perform a series of ligand docking experiments to delineate the architecture of the ligand-binding site. Structural models were created using homology modeling with the AChBP as a template. Docking of the antagonist granisetron was carried out using a Lamarckian genetic algorithm to produce models of ligand-receptor complexes. Two energetically similar conformations of granisetron in the binding site were obtained from the docking simulations. In one model, the indazole ring of granisetron is near W90 and the tropane ring near R92, while in the other, the orientation is reversed. We used double mutant cycle analysis to determine which of the two orientations is consistent with experimental data and find that the data are consistent with the model in which the indazole ring of granisetron interacts with R92 and the tropane ring interacts with W90. The combination of molecular modeling with double mutant cycle analysis offers a powerful approach for the delineation of the architecture of the ligand-binding site.

Molecular Pharmacology Fast Forward. Published on May 24, 2005 as DOI: 10.1124/mol.105.011957
This article has not been copyedited and formatted. The final version may differ from this version.

INTRODUCTION

The serotonin type 3 receptor (5-HT_3R) is a member of the cys-loop ligand-gated ion channel gene family, which includes the muscle and neuronal nicotinic acetylcholine receptors (AChR), the glycine receptor (GlyR), and the γ-aminobutyric acid type A ($GABA_A$R) receptor (Connolly and Wafford, 2004; Lester et al., 2004). Two different subunits, termed 5-HT_{3A} and 5-HT_{3B}, have been described (Reeves and Lummis, 2002). The 5-HT_{3A} subunit forms functional receptors with the appropriate pharmacological properties when expressed in *Xenopus* oocytes or mammalian cells. However there are some differences between the properties of the expressed homomeric receptors and 5-HT_3Rs in some, but not all, neurons. Perhaps the most significant difference is that the single-channel conductance of the expressed receptors is in the sub-pS range, while that of the receptors in many (but not all) neurons is in the 10-20 pS range (Hussy et al., 1994; Yang et al., 1992). This difference, along with the fact that other members of the cys-loop LGIC family are composed of several different subunits, led to the search and subsequent discovery of an additional 5-HT_3R subunit, now termed the 5-HT_{3B} subunit (Davies et al., 1999; Dubin et al., 1999).

When expressed by itself, the 5-HT_{3B} subunit does not form functional receptors. When the 5-HT_{3B} subunit is coexpressed with the 5-HT_{3A} subunit, the ligand-binding properties of the expressed receptors are identical to those resulting from expression of the 5-HT_{3A} subunit alone (Brady et al., 2001) and of

native 5-HT_3Rs. However, while homomeric 5-HT_{3A}Rs have single-channel conductances in the sub-picosiemen range, the heteromeric receptors (*i.e.,* 5-HT_{3A} + 5-HT_{3B} subunits) exhibit single channels with conductances of approximately 15 pS, just as seen in many neuronal 5-HT_3Rs (Davies et al., 1999; Dubin et al., 1999). Initial examination of the pattern of expression of the 5-HT_{3B} subunit showed that it was expressed in the same tissues and brain regions as the 5-HT_{3A} subunit, suggesting that all 5-HT_3Rs are heteromeric. However, subsequent expression profiling studies with better spatial resolution (reviewed in (van Hooft and Yakel, 2003)) have cast doubt on the notion that 5-HT_3Rs in the central nervous system are always heteromeric, so the question of subunit composition of "bona fide" 5-HT_3Rs is by no means settled. However, since the ligand-binding profiles of native, homomeric and heteromeric receptors are identical, the structure of the ligand-binding domain of the two types of expressed 5-HT_3Rs, as well as of native receptors, are highly similar. Thus, homomeric 5-HT_{3A}Rs should be an appropriate model for the structure of the ligand-binding domain of native 5-HT_3Rs.

Over the years, structural models for the 5-HT_{3A}R and other members of the ligand-gated ion channel family have been developed, mostly based on the extensive amount of data obtained from studies on the AChR (reviewed in (Karlin, 2002)), and then refined using mutagenesis data from the particular receptor under consideration. At first, these models were not of sufficient resolution to produce detailed models of the architecture of the ligand-binding domains, but the isolation and subsequent determination of the structure at

Molecular Pharmacology Fast Forward. Published on May 24, 2005 as DOI: 10.1124/mol.105.011957
This article has not been copyedited and formatted. The final version may differ from this version.

atomic resolution of a homologous acetylcholine-binding protein (AChBP) from the freshwater snail *Lymnea* (Brejc et al., 2001; Smit et al., 2001) has provided a true structure to use as a framework for constructing more realistic models of the extracellular domain of LGICs (Cromer et al., 2002; Le Novere et al., 2002; Maksay et al., 2003; Reeves et al., 2003).

In the case of AChBP-based models of the 5-HT_{3A}R (Maksay et al., 2003; Reeves et al., 2003), ligand-docking simulations produced several orientations of agonists (Reeves et al., 2003) or antagonists (Maksay et al., 2003) in the binding site, and the authors used data obtained from previous mutagenesis studies to evaluate models for consistency with experimental data in order to select feasible models for receptor-ligand interactions. In this report, rather than using previously-obtained data as the determinant of ligand-receptor model feasibility, we use the model itself to guide the design of experiments to test the model employing a variant of double-mutant cycle analysis (Hildago and MacKinnon, 1995). The results of these experiments can then be used to select the ligand-receptor model that is consistent with experimental data, and thus is most likely to be correct.

Molecular Pharmacology Fast Forward. Published on May 24, 2005 as DOI: 10.1124/mol.105.011957
This article has not been copyedited and formatted. The final version may differ from this version.

MATERIALS AND METHODS

Molecular Biology and Transfection:

A full length cDNA clone corresponding to the 5-$HT_{3A(b)}$ form (Hope et al., 1993) of the receptor was isolated from a neuroblastoma N1E-115 cell line cDNA library as previously described (Yan et al., 1999) and subcloned into vector pCI (Promega, Madison, WI). Site-directed mutagenesis was carried out using the QuickChange system (Stratagene, La Jolla, CA) as described previously (Yan et al., 1999). The nomenclature used to describe mutants is amino acid in wild-type/position/substitution; *e.g.,* W90F. Because the amino terminus of the mature 5-HT_{3A} subunit is unknown, the amino acid numbering system here includes the signal sequence and has the initial methionine as position 1. Please note that the numbering system for the 5-HT_{3A} receptor used in a previous study from this laboratory has changed somewhat so that the W90F and R92A mutations in this study correspond to the W89F and R91A mutations, respectively, in the original study (Yan et al., 1999). Cultures of tsA201 cells, a derivative of the widely-used HEK 293 cell line, were maintained in DMEM medium containing 10% fetal bovine serum, 100 units/ml penicillin and 100 units/ml streptomycin. Cultures at 30-40% confluence were transfected with 20 μg receptor cDNA per 100 mm dish using the calcium phosphate technique (Wigler et al., 1979). After 12 hours exposure to the DNA/calcium phosphate solution, the medium was replaced with fresh medium and the cells were allowed to grow for another 24-36 hours prior to use. Maximal expression was obtained 36-72 hours after transfection.

Ligand binding assays:

Molecular Pharmacology Fast Forward. Published on May 24, 2005 as DOI: 10.1124/mol.105.011957
This article has not been copyedited and formatted. The final version may differ from this version.

Transfected cells were scraped from dishes, washed three times with phosphate buffered saline and resuspended and homogenized in 2.5 ml 154 mM NaCl, 50 mM Tris-HCl, pH 7.4 per 100 mm dish. The homogenate was then used in binding assays or frozen until needed. We observed no change in either ligand affinity or B_{max} values after freezing.

Membranes were incubated for 2 hours at 37º in a total volume of 0.5 ml 154 mM NaCl, 50 mM TrisHCl, pH 7.4 containing the appropriate concentrations of antagonist and radioligand ([^{3}H] granisetron; New England Nuclear, 85 Ci/mmol). Binding was terminated by rapid vacuum filtration onto GF/B filters that had been pretreated with 50 mM TrisHCl, pH 7.4, 0.2% polyethyleneimine and the filters were washed with 10 ml cold 50 mM TrisHCl, pH 7.4 per sample. Nonspecific binding was defined as that binding not displaced by 100 μM *m*-chlorophenyl biguanide. IC_{50} values for various antagonists were determined by fitting the data to Eq. 1 using a Levenberg-Marquardt algorithm in a commercially available software package for Macintosh computers (Igor Pro, WaveMetrics, Oswego, OR):

$$\theta = (1 + ([I]/IC_{50})^{n})^{-1} \quad (1)$$

where θ is the fractional amount of [^{3}H] granisetron bound in the presence of the antagonist at concentration [I] compared to that in the absence of antagonist, IC_{50} is the concentration of antagonist at which θ=0.5, and *n* is the apparent Hill coefficient. K_i values were calculated from the IC_{50} values and the K_d for [^{3}H] granisetron using the Cheng-Prusoff relation (Cheng and Prusoff, 1973) (Eq. 2.):

$$K_i = \frac{IC_{50}}{1 + ([L]/K_d)} \quad (2)$$

Molecular Pharmacology Fast Forward. Published on May 24, 2005 as DOI: 10.1124/mol.105.011957
This article has not been copyedited and formatted. The final version may differ from this version.

where [L] is the concentration of [^{3}H]granisetron used to determine the IC_{50} value in the experiment and K_d is the dissociation constant for [^{3}H]granisetron. For the Cheng-Prusoff relation to be applicable, the Hill coefficient for the IC_{50} curve must be equal to 1. In our experiments, all Hill coefficients were not statistically different from unity at a 95% confidence level (data not shown). In this study, all experiments were carried out with a [^{3}H]granisetron concentration equal to its experimentally-determined dissociation constant for the particular receptor (WT: 2.1 nM; W90F: 28.6 nM; R92A: 13.6 nM (Table 1)), meaning that the IC_{50} values were twice the K_i.

Ligands

The structures of the ligands used in this study are shown in Figure 3. [^{3}H]granisetron was obtained from New England Nuclear, MDL 72222 from Sigma (St. Louis), and ondansetron from Glaxo Research (United Kingdom).

Molecular Modeling

A structural model of the extracellular domain of the mouse $5HT_{3A}R$ was generated using version 7.7 of the program MODELLER (Sali and Blundell, 1993), using the X-ray structure of AChBP as template (Protein Data Bank ID:1I9B, (Brejc et al., 2001)). The sequence alignment between AChBP and $5HT_{3A}R$ monomers was performed with Align2D from the MODELLER suite , which uses a variable gap opening penalty that depends on the three-dimensional structure of the template. All five subunits were modeled

simultaneously to ensure structural integrity between subunits at their interfaces. All polar hydrogens, but not nonpolar hydrogens, were included to allow for main-chain hydrogen bonding. The programs PROCHECK and ProSa2003 were used to evaluate the generated models (Laskowski et al., 1993; Sippl, 1993), and the model that ranked highest by PROCHECK and ProSa2003 was chosen for ligand docking.

Ligand Docking Simulations

$5HT_3R$ ligands were docked to each binding site in the chosen model using Autodock 3.0 (Morris et al., 1998). Solvation parameters were added to the protein coordinate file and the ligand torsions were defined using the 'Addsol' and 'Autotors' utilities, respectively, in Autodock 3.0. Gasteiger-Marsili charges were applied to ligands prior to docking (Gasteiger and Marsili, 1980), which uses the united atom representation for nonpolar hydrogens. The docking was performed with the initial population size set to 100 with 100 independent runs using otherwise default parameters in the standard protocol on a 30x30x40 Å grid with spacing of 0.375 Å. The size of the grid gives sufficient freedom for the ligands to be docked in all possible orientations while not permitting them move outside of the binding site. In addition to returning the docked structure, AutoDock also calculates an affinity constant for each ligand-receptor configuration. Images of the receptor with and without docked ligands were produced using the UCSF Chimera package (Pettersen et al., 2004) from the Computer Graphics

Laboratory, University of California, San Francisco (supported by NIH P41 RR-01081).

Molecular Pharmacology Fast Forward. Published on May 24, 2005 as DOI: 10.1124/mol.105.011957
This article has not been copyedited and formatted. The final version may differ from this version.

RESULTS

The extracellular domain of the 5-HT_{3A}R was modeled using the known three-dimensional structure of the acetylcholine binding protein (AChBP) from *Lymnea* (Brejc et al., 2001) as a template for homology modeling using MODELLER (Figure 1;(Sali and Blundell, 1993)). As with models for the 5-HT_{3A}R reported previously (Maksay et al., 2003; Reeves et al., 2003), each subunit assumes an immunoglobulin-like fold structure (Figure 1). In the AChBP, and, by inference, the other members of the cys-loop ligand-gated ion channel family, the ligand-binding domain is at the interface between subunits and is made up of a series of six domains (A-F), three from one subunit (A-C), and three from the adjacent subunit (D-F) (Brejc et al., 2001; Celie et al., 2004). Consistent with this notion, studies from several laboratories have identified a number of residues at or near the 5-HT_3R ligand-binding site (Boess et al., 1997; Hope et al., 1999; Price and Lummis, 2004; Schreiter et al., 2003; Spier and Lummis, 2000; Venkataraman et al., 2002; Yan et al., 1999; Yan and White, 2002) which are located in the various binding-site domains in the model.

We used a Lamarckian genetic algorithm (AutoDock; (Morris et al., 1998)) to create models of antagonist-receptor interactions within the ligand-binding domain using granisetron as the ligand. The models of the 5-HT_{3A}R/granisetron complex produced by this procedure fall into two broad classes (Fig. 2; Table 1)-those with the indazole ring of granisetron near W90, and those with the indazole ring near R92. Given the various assumptions that underlie the calculations

Molecular Pharmacology Fast Forward. Published on May 24, 2005 as DOI: 10.1124/mol.105.011957
This article has not been copyedited and formatted. The final version may differ from this version.

involved in the docking process, using the calculated K_i's to discriminate between models is not appropriate, especially when the K_i's are very close together.

Double-mutant cycle analysis (Carter et al., 1984) can be used to determine whether or not a particular residue interacts with a particular portion of a ligand. The underlying logic of this approach is that if residue *x* in the binding site interacts with residue *y* on the ligand, then the effect of mutating *x* should depend upon whether residue *y* in the ligand is changed or not. An interaction parameter, Ω, is calculated from the K_d or K_i values as

$$\Omega = \frac{(K_{W,L1}/K_{W,L2})}{(K_{m,L1}/K_{m,L2})} \quad \text{(Eq. 3)}$$

where the subscripts indicate the following: *W* for wild-type receptor, *m* for mutant receptor, and *L1* and *L2* for the two ligands being compared. An Ω value significantly different from 1 indicates an interaction between the functional group on the ligand and the amino acid on the receptor. Although initially used for analysis of the interaction of peptide toxins with K^+ channels (Hildago and MacKinnon, 1995), this approach has also been applied to identify points of contact between AChRs and peptide toxins (Malany et al., 2000) and AChRs and *d*-tubocurarine analogs (Willcockson et al., 2002).

We have used the interaction of three different ligands (granisetron, MDL 72222, and ondansetron; Figure 3) with wild-type, W90F, and R92A receptors to evaluate the models produced in the docking simulations. These two residues (W90 and R92) are in loop D of the binding site, and we have previously shown that they play a role in ligand-receptor interactions (Yan et al., 1999). To a crude approximation, MDL 72222 and ondansetron can be thought of as being

Molecular Pharmacology Fast Forward. Published on May 24, 2005 as DOI: 10.1124/mol.105.011957
This article has not been copyedited and formatted. The final version may differ from this version.

structural variants of granisetron. In the case of MDL 72222, the indazole ring of granisetron is "mutated" to a chlorobenzoyl ring, while in the case of ondansetron, the tropane ring of granisetron is "mutated" to an imidazole ring. Figure 4 shows the inhibition of [^{3}H]granisetron binding to wild-type, W90F, and R92A receptors by MDL 72222. The W90F mutation markedly reduces the affinity for MDL 72222, while the R92A mutation slightly increases affinity for the receptor. Table 2 shows the results of the analysis of the interaction of all three ligands with all three receptors. The W90F mutation reduces the affinity for each ligand, while the R92A mutation reduces the affinity of granisetron and ondansetron, but increases the affinity for MDL 72222.

The combination of three receptors (wild-type, W90F, and R92A) and three ligands (granisetron, MDL 72222, and ondansetron) gives rise to four double-mutant cycles: (a) WT/W90F/granisetron/MDL 72222, (b) WT/W90F/granisetron/ondansetron, (c) WT/R92A/granisetron/MDL 72222, and (d) WT/R92A/granisetron/ondansetron. For each cycle, an interaction parameter, Ω, can be calculated from estimates of the K_d (granisetron) and K_i (MDL 72222 and ondansetron) values of the relevant receptors. Figure 5 shows the four double-mutant cycles that can be constructed, along with the corresponding Ω values. Only two of the cycles have Ω values different than 1.0. The WT/R92A/granisetron/MDL 72222 cycle has an Ω value of 10.8 and the WT/W90F/granisetron/ondansetron cycle has an Ω value of 2.2. When the structures of the three ligands are examined, these data suggest that the indazole ring of granisetron interacts with R92 and the tropane ring of granisetron

Molecular Pharmacology Fast Forward. Published on May 24, 2005 as DOI: 10.1124/mol.105.011957
This article has not been copyedited and formatted. The final version may differ from this version.

interacts with W90. These data can be used to evaluate the ligand-receptor models obtained from the modeling studies, as will be described below.

DISCUSSION

The ultimate goal of molecular modeling is to produce a model that accurately represents the three-dimensional structure of the protein under study. In cases where actual structural data are missing, homology-based models using the structures of related proteins have proven to be a useful approach. In the case of cys-loop LGICs, workers have used the structure of the *Lymnea* AChBP as a template upon which to build structural models of the extracellular (*i.e.,* ligand-binding) domain of the receptors, and then evaluated the models in light of previously-obtained mutagenesis data. Using this approach, two groups have produced models of the 5-HT_{3A}R binding site (Maksay et al., 2003; Reeves et al., 2003). Although the lack of publicly-available PDB coordinate files of these other two models precludes a detailed comparison of our model with the other two, the backbone structures of these models are similar to ours, but there are undoubtedly differences in the orientation of side chains within the structures.

The ligand-docking simulations with the antagonist granisetron produced four clusters of docked structures with calculated K_i's in the 2-6 nM range, similar to the experimentally-obtained K_i value for wild-type receptors. Three of the models (clusters 1-3; Table 1, Figure 2A)) have granisetron oriented in the binding site such that the indazole ring of granisetron is near W90 and the tropane ring is near R92, while the fourth (cluster 4; Figure 2B) has the opposite orientation. Maksay *et al.* (Maksay et al., 2003) carried out docking simulations with granisetron with the human, mouse, and guinea pig 5-HT_{3A}R. They produced several models of the granisetron-receptor complex, and the lowest

energy model was one in which the tropane ring of granisetron was near W90 and the indazole ring was closer to R92, similar to our cluster 4; other, higher-energy models had the opposite orientation, similar to our clusters 1-3. However, the authors did not provide information on the either the values of the energies or calculated K_i's, so it is not possible to determine the energy relationships of the different reported conformations.

Given that the calculated K_i's of the four clusters of structures that were produced in this study are very close to each other, choosing one granisetron orientation over the others based solely on calculated K_i values is inappropriate. We chose to test the models using double-mutant cycle analysis. This type of analysis can be used to determine whether or not a particular residue interacts with a particular portion of a ligand; *i.e.*, which parts of a ligand are in close physical proximity to a particular residue. By using three different ligands (granisetron, MDL 72222, and ondansetron), we were able to examine both "halves" of the ligand. The Ω value for the WT/R92A/granisetron/MDL 72222 cycle suggests that the indazole ring of granisetron, but not the tropane ring, interacts with R92, while the Ω value for the WT/W90/granisetron/ondansetron cycle suggests that the tropane ring, but not the indazole ring, interacts with W90. Note that the use of the three different ligands provides an internal check for the consistency of the results; *i.e.*, two independent cycles with Ω values >1 lead to the same conclusion regarding the orientation of granisetron in the binding site. Thus, although the orientation of granisetron in cluster 4 is not as energetically favorable as the others (at least based on calculations), it is the only

orientation that is consistent with the double-mutant cycle data, strongly suggesting that this is the actual orientation of granisetron in the ligand-binding site.

The values of Ω from the double-mutant cycle analysis are associated with rather low $\Delta\Delta G$ values (approximately -1.4 kcal/mol for the WT/R92A/granisetron/MDL 72222 cycle, and approximately -0.5 kcal/mol for the WT/W90/granisetron/ondansetron cycle), indicating that the interactions are quite weak, due to the type interaction (such as van der Waal's or hydrogen bonds) and/or the distance over which the interaction occurs. Similarly weak interactions were observed in a double-mutant cycle analysis of the interaction of *d*-tubocurarine with the nicotinic acetylcholine receptor (Willcockson et al., 2002).

Reeves *et al.* (Reeves et al., 2003) developed a homology-based model of the 5-HT_3R and carried out docking simulations using serotonin as the ligand. Seven different orientations of 5-HT in the binding site were obtained. In the two orientations that they chose as most likely, the amino group of the indole ring of 5-HT was close to W90, but no part of the agonist was near enough to R92 to suggest that an interaction formed between R92 and the agonist. In other, less-favored orientations, the hydroxyl group of 5-HT was in a pocket containing R92, and the side chain amine was near W90. However, none of the models put the indole ring near R92. If the indazole ring of granisetron makes interactions similar to those made by the indole ring of 5-HT, then based upon our model, we would expect that the indole of 5-HT would be near R92, which none of the agonist-receptor models show. One possible non-trivial explanation for this is that due to

the allosteric nature of ligand-induced channel gating, agonists and antagonists interact with different conformations of the binding site. Thus, one may not expect identical interactions to be observed for agonists and antagonists.

In the present study we used double-mutant cycle analysis to evaluate various docked orientations of antagonists. Unfortunately, the fact that agonists induce conformational changes in the receptor make it impossible to obtain accurate estimates of agonist affinity of wild-type and mutant receptors using ligand-binding assays (Colquhoun, 1998). As a result, one cannot evaluate models of agonist-receptor interaction using the experimental approach done here. In the absence of a rigorous method of testing proposed structures of agonist-receptor complexes, extension of our model to agonist-receptor interactions is premature at present.

This study shows the power of double-mutant cycle analysis with small molecule ligands of differing structure to probe ligand-receptor interactions in a way that can map differing portions of the ligand onto specific regions of the receptor. In conjunction with molecular modeling studies, an iterative loop of modeling and experimental testing of models can be created that can accelerate the process of elucidating the three-dimensional architecture of a ligand-binding domain. Inclusion of a wide variety of ligands and mutant receptors, should allow the examination of the architecture of the entire ligand-binding domain, and thus provide useful information for the design of novel pharmacological agents with both high affinity and high specificity for use as therapeutic agents.

REFERENCES

Boess F, Steward L, Steele J, Liu D, Reid J, Glencorse T and Martin I (1997) Analysis of the ligand binding site of the 5-HT_3 receptor using site directed mutagenesis: Importance of Glutamate 106. *Neuropharmacology* **36**:637-647.

Brady C, Stanford I, Ali I, Lin L, Williams J, Dubin A, Hope A and Barnes N (2001) Pharmacological comparison of human homomeric 5-HT_{3A} receptors versus heteromeric 5-$HT_{3A/3B}$ receptors. *Neuropharmacology* **41**:282-284.

Brejc K, van Dijk W, Klaassen R, Schuurmans M, van der Oost J, Smit A and Sixma T (2001) Crystal structure of an ACh-binding protein reveals the ligand-binding domain of nicotinic receptors. *Nature* **411**:269-276.

Carter P, Winter G, Wilkinson A and Fersht A (1984) The use of double mutants to detect structural changes in the active site of tyrosyl-tRNA synthetase (Bacillus stearothermophilus). *Cell* **38**:835-840.

Celie P, van Rossum-Fikkert S, van Dijk W, Brejc K, Smit A and Sixma T (2004) Nicotine and carbamylcholine binding to nicotinic acetylcholine receptors as studied in AChBP crystal structures. *Neuron* **41**:907-914.

Cheng Y and Prusoff W (1973) Relationship between inhibition constant (K_i) and the concentration of inhibitor which causes 50 percent inhibition (IC_{50}) of an enzymatic reaction. *Biochem Pharmacol* **22**:3099-3108.

Colquhoun D (1998) Binding, gating, affinity and efficacy: The interpretation of structure-activity relationships for agonists and the effects of mutating receptors. *Br J Pharmacol* **125**:924-947.

Connolly C and Wafford K (2004) The cys-loop superfamily of ligand-gated ion channels; The impact of receptor structure on function. *Biochem Soc Trans* **32**:529-534.

Cromer B, Morton C and Parker M (2002) Anxiety over $GABA_A$ receptor structure relieved by AChBP. *Trends Biochem Sci* **27**:280-287.

Davies P, Pistis M, Hanna M, Peters J, Lambert J, Hales T and Kirkness E (1999) The 5HT3B subunit is a major determinant of serotonin receptor function. *Nature* **397**:359-363.

Dubin A, Huvar R, D'Andrea M, Pyati J, Zhu J, Joy K, Wilson S, Galindo J, Glass C, Luo L, Jackson M, Lovenberg T and Erlander M (1999) The pharmacological and functional characteristics of the serotonin 5-HT_{3A} receptor are specifically modified by a 5-HT_{3B} receptor subunit. *J Biol Chem* **274**:30799-30810.

Gasteiger J and Marsili M (1980) Iterative partial equalization of orbital electronegativity- A rapid access to atomic charges. *Tetrahedron* **36**:3219-3228.

Hildago P and MacKinnon R (1995) Revealing the architecture of a K^+ channel pore through mutant cycles with a peptide inhibitor. *Science* **268**:307-310.

Hope A, Belelli D, Mair ID, Lambert J and Peters J (1999) Molecular determinants of (+)-tubocurarine binding at recombinant 5-hydroxytryptamine$_{3A}$ receptor subunits. *Mol Pharmacol* **55**:1037-1043.

Hope A, Downie D, Sutherland L, Lambert J, Peters J and Burchell B (1993) Cloning and functional expression of an apparent splice variant of the murine 5-HT_3 receptor A subunit. *Eur J Pharmacol* **245**:187-192.

Hussy N, Lukas W and Jones K (1994) Functional properties of a cloned 5-hydroxytryptamine ionotorpic receptor subunit: comparison with native mouse receptors. *J Physiol (Lond)* **481**:311-323.

Karlin A (2002) Emerging structure of the nicotinic acetylcholine receptor. *Nat Rev Neurosci* **3**:102-114.

Ku H (1966) Notes on the use of propagation of error formulas. *J. Res. Nat. Bur. Standards C. Engineering and Instrumentation* **70C**:263-273.

Laskowski R, MacArthur M, Moss D and Thorton J (1993) PROCHECK: A program to check the stereochemical quality of protein structures. *J Appl Crystallogr* **26**.

Le Novere N, Grutter T and Changeux J-P (2002) Models of the extracellular domain of the nicotinic receptors and of agonist- and Ca^{++}-binding sites. *Proc Natl Acad Sci USA* **99**:3210-3215.

Lester H, Dibas M, Dahan D, Leite J and Dougherty D (2004) Cys-loop receptors: New twists and turns. *Trends Neurosci* **27**:329-336.

Maksay G, Bukadi Z and Simonyi M (2003) Binding interactions of antagonists with 5-hydroxytryptamine3A receptor models. *J Recept Signal Transduct Res* **23**:255-270.

Malany S, Osaka H, Sine S and Taylor P (2000) Orientation of α-neurotoxin at the subunit interfaces of the nicotinic acetylcholine receptor. *Biochemistry* **39**:15388-15398.

Morris G, Goodsell D, RS H, Huey R, Hart W, Belew R and Olson A (1998) Automated docking using Lamarckian genetic algorithm and an empirical free energy binding free energy function. *J Comp Chem* **19**:1639-1662.

Pettersen E, Goddard T, Huang C, Couch G, Greenblatt D, Meng E and Ferrin T (2004) UCSF Chimera: A visualization system for exploratory research and analysis. *J Comput Chem* **25**:1605-1612.

Price K and Lummis S (2004) The role of tyrosine residues in the extracellular domain of the 5-HT_3 receptor. *J Biol Chem* **279**:23294-23301.

Reeves D and Lummis S (2002) The molecular basis of the structure and function of the 5-HT3 receptor:A model ligand-gated ion channel. *Mol Membr Biol* **19**:11-26.

Reeves D, Sayed M, Chau P-L, Price K and Lummis S (2003) Prediction of 5-HT_3 receptor agonist-binding residues using homology modeling. *Biophys J* **84**:2338-2344.

Sali A and Blundell T (1993) Comparitive protein modeling by satisfaction of spatial restraints. *J Mol Biol* **234**:779-815.

Schreiter C, Hovius R, Costioli M, Pick H, Kellenberger S, Schild L and Vogel H (2003) Characterization of the ligand-binding site of the serotonin 5-HT_3 receptor: The role of glutamate residues 97,224,and 235. *J Biol Chem* **278**:22709-22716.

Sippl M (1993) Recognition of errors in three-dimensional structures of proteins. *Proteins* **17**:355-362.

Smit A, Syed N, Schaap D, van Minnen J, Klumperman J, Kits KS, Lodder H, van der Schors R, van Elk R, Sorgedrager B, Brejc K, Sixma T and Geraerts W (2001) A glia-derived acetylcholine-binding protein that modulates synaptic transmission. *Nature* **411**:261-268.

Spier A and Lummis S (2000) The role of tryptophan residues in the 5-Hydroxytryptamine(3) receptor ligand binding domain. *J Biol Chem* **275**:5620-5.

van Hooft J and Yakel J (2003) 5-HT_3 receptors in the CNS:3B or not 3B? *Trends Pharmacol Sci* **24**:157-160.

Venkataraman P, Ventakatachalan S, Joshi P, Muthalagi M and Schulte M (2002) Identification of critical residues in loop E of the 5-HT_{3AS}R binding site. *BMC Biochem* **3**:15.

Wigler M, Sweet R, Sim G, Wold B, Pellicer A, Lacy E, Maniatis T, Silverstein S and Axel R (1979) Transformation of mammalian cells with genes from procaryotes and eucaryotes. *Cell* **16**:777-785.

Willcockson I, Hong A, Whisenant R, Edwards J, Wang H, Sarkar H and Pedersen S (2002) Orientation of *d*-tubocurarine in the muscle nicotinic acetylcholine receptor-binding site. *J Biol Chem* **277**:42249-42258.

Yan D, Schulte M, Bloom K and White M (1999) Structural features of the ligand-binding domain of the serotonin 5HT_3 receptor. *J Biol Chem* **274**:5537-5541.

Yan D and White M (2002) Interaction of *d*-tubocurarine analogs with mutant 5-HT_3 receptors. *Neuropharmacology* **43**:367-373.

Yang J, Mathie A and Hille B (1992) 5-HT_3 receptor channels in dissociated rat superior cervical ganglion neurons. *J Physiol (Lond)* **448**:237-256.

FOOTNOTES

This work was supported by a grant from the American Heart Association Pennsylvania-Delaware Affiliate.

LEGENDS FOR FIGURES

Figure 1: Structural model of the extracellular domain of the $5HT_{3A}R$. (A) Top view of the pentamer. (B) Side view of a subunit-subunit interface, with the putative loops in the binding domains (A-F) in color: A: red; B: cyan; C :orange; D: magenta; E: yellow; F: green.

Figure 2: Granisetron docked in the ligand-binding site. Two representative models of granisetron docked in the ligand-binding domain between two subunits are shown. The 5-$HT_{3A}R$ subunits are shown as ribbon figures with W90, R92, and granisetron labeled and shown as space-filling structures. In models from clusters 1, 2, and 3 (A), the indazole ring of granisetron is near W90 and the tropane ring is near R92, while in models from cluster 4 (B), the orientation of granisetron is flipped.

Figure 3: Structure of ligands used in this study. Note that each ligand can be considered to consist of two "halves"- granisetron: indazole/tropane; MDL 72222: chlorobenzoyl/tropane; and ondansetron: indole/imidazole.

Figure 4: Effects of W90F and R92A mutations on MDL 72222 affinity. The concentration dependences of inhibition of [^{3}H] granisetron binding by MDL 72222 to wild-type (●), W90F (■), and R92A (▲) 5-HT_{3A}Rs are shown. Each data point represents the mean $\pm$ S.E.M. of 3 determinations. The solid curves are drawn according to Equation 1 with IC_{50} values of 25 nM (wild-type), 500 nM

(W90F), and 15 nM (R92A). Note that the W90F mutation decreases MDL 72222 affinity, while the R92A mutation increases affinity.

Figure 5: Double-mutant cycles for WT, W90F, and R92A receptors and granisetron, MDL 72222, and ondansetron. The interaction coefficient, Ω, for all combinations of the three ligands (granisetron, MDL 72222, and ondanstron) with the three receptors (WT, W90F, and R92A) was determined from the K_d or K_i values of each ligand for each receptor. Error estimates were obtained through analysis of propagation of errors (Ku, 1966). The Ω value of 10.8 for the WT/R92A and granisetron/MDL 72222 cycle indicates that R92 interacts with the indazole ring of granisetron, while the Ω value of 2.2 for the WT/W90F and granisetron/ondansetron indicates that W90F interacts with the tropane ring of granisetron.

Molecular Pharmacology Fast Forward. Published on May 24, 2005 as DOI: 10.1124/mol.105.011957
This article has not been copyedited and formatted. The final version may differ from this version.

TABLES

Table 1: Granisetron orientation in docked models

Cluster	frequency	K_i, nM	at indazole	at tropane
1	0.6	2.6	W90	R92
2	0.2	3.4	W90	R92
3	0.1	4.6	W90	R92
4	0.1	5.5	R92	W90

Legend: Docking simulations were carried out using AutoDock as described in the Methods section. The orientation of granisetron in the binding site of the four clusters with highest affinity was examined to determine which portions of the ligand were near W90 and R92.

Molecular Pharmacology Fast Forward. Published on May 24, 2005 as DOI: 10.1124/mol.105.011957
This article has not been copyedited and formatted. The final version may differ from this version.

Table 2: Affinity of ligands for WT and mutant receptors

Receptor	Ligand	K_d or K_i, nM
WT	granisetron	2.3 ± 0.8
W90F	granisetron	43.3 ± 2.1*
R92A	granisetron	13.6 ± 0.4*
WT	MDL 72222	11.1 ± 0.7
W90F	MDL 72222	215.9 ± 24.9*
R92A	MDL 72222	5.9 ± 0.6*
WT	ondansetron	3.0 ± 1.3
W90F	ondansetron	121.2 ± 6.2*
R92A	ondansetron	15.6 ± 2.5*

Legend: Estimates of K_d values for granisetron were determined from saturation binding experiments using [^{3}H] granisetron and K_i values for MDL 72222 and ondansetron were calculated from experimentally-determined IC_{50} values for the inhibition of [^{3}H] granisetron binding to wild-type or mutant receptors as described in the Methods section. Each value represents the mean ± S.E.M. of 3 separatedeterminations. Values for the mutant receptors marked with * are statistically different from wild-type at a 95% confidence level using Student's *t* test.

1

2

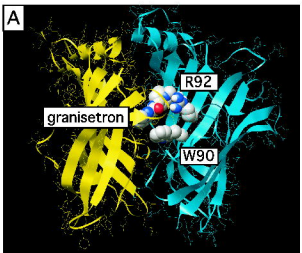

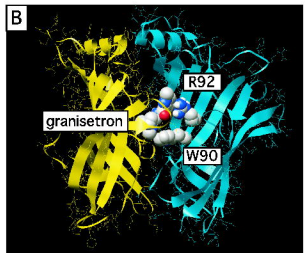

3

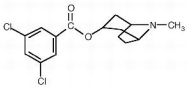

MDL-72222

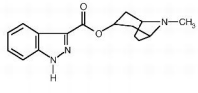

Granisetron

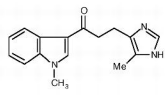

Ondansetron

4

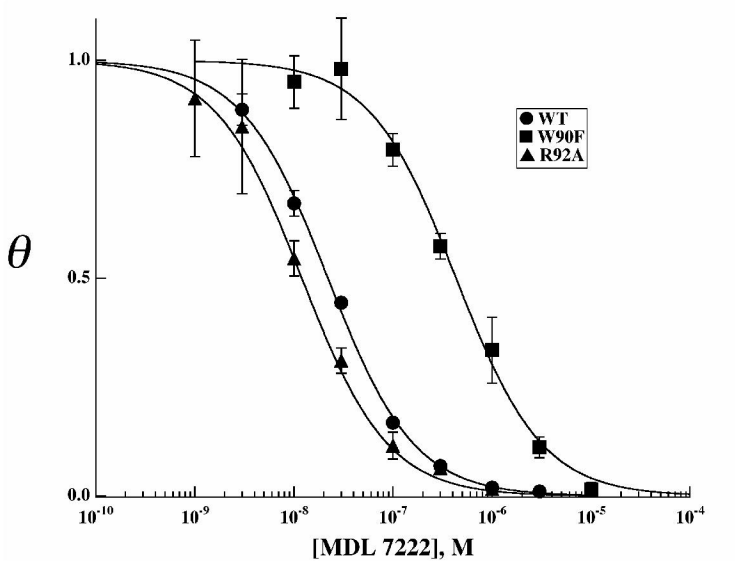

5

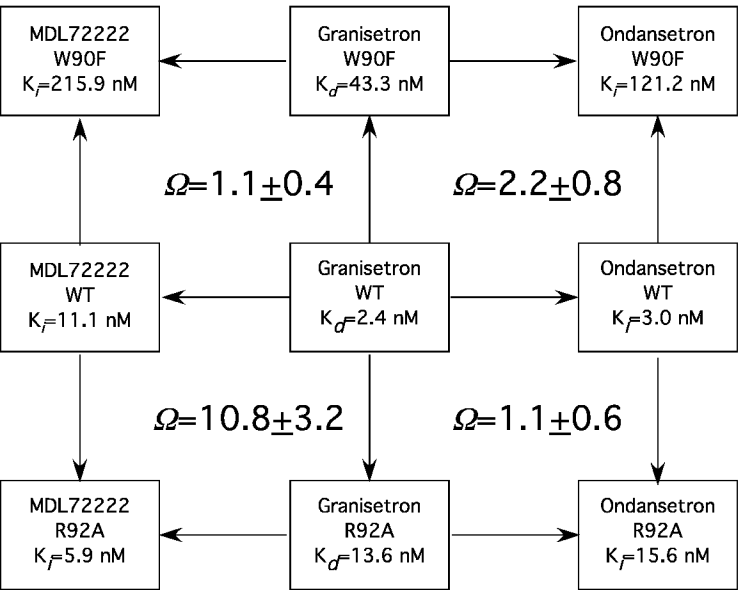
MDL72222
W90F
K_i=215.9 nM
Granisetron
W90F
K_d=43.3 nM
Ondansetron
W90F
K_i=121.2 nM
Ω=1.1±0.4
Ω=2.2±0.8
MDL72222
WT
K_i=11.1 nM
Granisetron
WT
K_d=2.4 nM
Ondansetron
WT
K_i=3.0 nM
Ω=10.8±3.2
Ω=1.1±0.6
MDL72222
R92A
K_i=5.9 nM
Granisetron
R92A
K_d=13.6 nM
Ondansetron
R92A
K_i=15.6 nM